

Article

A 7-Hydroxybenzoxazinone-Containing Fluorescence Turn-On Probe for Biothiols and Its Bioimaging Applications

Bin Li, Datong Zhang *, Ruibing An and Yaling Zhu

School of Chemistry and Pharmaceutical Engineering, Qilu University of Technology (Shandong Academy of Sciences), 3501 Daxue Road, Jinan 250353, China

* Correspondence: dtzhang@qlu.edu.cn; Tel.: +86-531-89631208

Academic Editor: Evangelos Gikas

Received: 5 August 2019; Accepted: 26 August 2019; Published: 27 August 2019



Abstract: In this work, a novel 7-hydroxybenzoxazinone-based fluorescent probe (**PBD**) for the selective sensing of biothiols is reported. Upon treatment with biothiols, **PBD** shows a strong fluorescence enhancement (up to 70-fold) and a large Stokes shift (155 nm). Meanwhile, this probe exhibits high resistance to interference from other amino acids and competing species. **PBD** features good linearity ranges with a low detection limit of 14.5 nM for glutathione (GSH), 17.5 nM for cysteine (Cys), and 80.0 nM for homocysteine (Hcy), respectively. Finally, the potential utility of this probe for biothiol sensing in living HeLa cells is demonstrated.

Keywords: fluorescence probe; biothiols; 7-hydroxy-3-phenyl-benzoxazinone; large Stokes shift; 2,4-dinitrobenzenesulfonate

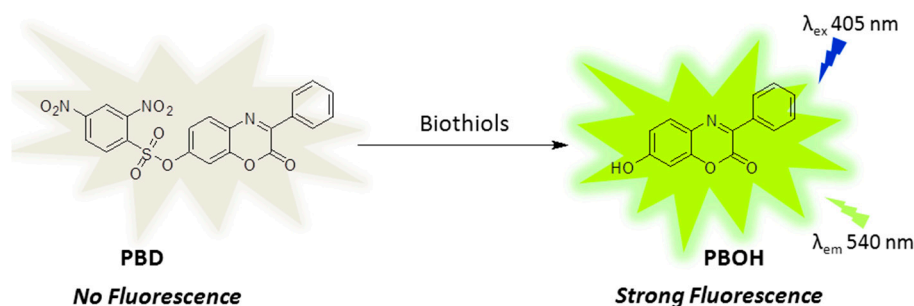
1. Introduction

Sulfhydryl-containing amino acids, such as cysteine (Cys), glutathione (GSH), and homocysteine (Hcy), play key roles in maintaining appropriate physiological and biological processes [1–5]. Malfunction of Cys levels has been associated with hair depigmentation, slowed growth rate, liver damage, edema, and so on [6]. Elevated levels of Hcy result in cardiovascular and Alzheimer’s disease [7,8]. GSH is the most abundant intracellular non-protein thiol and its concentration is within millimolar range. GSH deficiency is linked with cancer, liver damage, and neurodegenerative disease [9–11]. Owing to their significant roles, it is of great importance to develop rapid, simple and reliable methods for monitoring the levels of biothiols in biological systems.

Among various detection methods, fluorescent-probe-based detection has been accepted as one of the most efficient methods due to its advantages of having operational simplicity, being low cost, working under in situ real time conditions and involving no invasive bioimaging [12–16].

Great efforts have been directed to the development of fluorescent probes toward biothiols (Cys, Hcy, and GSH) [17–23]. Many probes have been constructed based on traditional fluorescent dyes, such as fluorescein [24], naphthalimide [25], coumarin [26], cyanin [27], BODIPY (boron-dipyrrromethene) [23], xanthene [28], 2-(2'-hydroxyphenyl)benzothiazole [29], and dicyanomethylene-4*H*-pyran derivatives [30]. In spite of some sensors with good sensing performance, many of these probes still suffer from poor solubility, low sensitivity, low quantum yield, and a time-consuming detection process. Thus, it would be beneficial to develop fluorophores with a new structural skeleton. Up until now, fluorescent dyes with a 7-hydroxybenzoxazinone skeleton have received little attention [31–33]. We prepared 7-hydroxy-3-phenylbenzoxazinone (**PBOH**) and evaluated its optical property. **PBOH** exhibits strong yellow-green fluorescence and a large Stokes shift (155 nm). We envisioned that masking the hydroxyl group in **PBOH** with a 2,4-dinitrophenylsulfonyl

group (DNBS) could generate a new fluorescent probe (**PBD**) for the selective detection of biothiols (Scheme 1). As they are well-known, arenesulfonates and arenesulphonamides can be readily cleaved by thiolate anions, and, therefore, the 2,4-dinitrobenzenesulfonyl (DNBS) group has often been chosen as the trigger group for thiols [24,34–38]. More importantly, the DNBS group can totally quench fluorescence, thus reducing background interference, because of its strong electron-withdrawing ability. We speculate that biothiols induce cleavage of the ester bond in the DNBS-PBOH conjugates, which can release free **PBOH** and thereby restore the strong emission, thus realizing a selective fluorescence off-on recognition of biothiols. The new probe **PBD** indeed exhibits a significant off-on response to biothiols. The investigation of **PBD** suggested that it possesses a strong anti-interference ability while sensing biothiols, with a low detection limit of 14.5 nM for GSH, 17.5 nM for Cys, and 80.0 nM for Hcy, respectively. In addition, **PBD** was successfully applied for biothiol detection in living HeLa cells.



Scheme 1. Design diagram of fluorescent probe **PBD** (2,4-dinitrobenzenesulfonate of 7-hydroxy-3-phenylbenzoxazinone) for biothiol detection.

2. Results and Discussion

PBOH showed strong fluorescence ($\Phi = 0.60$) with a maximum at 540 nm and an absorption band centered at 385 nm in EtOH-PBS buffer (Phosphate Buffered Saline) solution (10 mM, pH = 7.4, 4:6, *v/v*) (Stokes shift = 155 nm). Owing to the quenching effect of the DNBS group, **PBD** alone exhibited extremely weak fluorescence with a low quantum yield at 540 nm ($\Phi = 0.011$), and its absorption maximum was blue-shifted to 340 nm under the same aqueous conditions (Figure S1). As expected, upon addition of biothiols, a remarkable fluorescence intensity enhancement at 540 nm was observed. As such, we constructed a turn-on fluorescent probe for biothiols.

2.1. Time-Dependence and pH Effect

The sensory effect of **PBD** is exemplified by its reaction with GSH. The emission intensity was recorded at different time points to evaluate the response time between **PBD** and various amounts of GSH. As shown in Figure 1, after addition of GSH, the fluorescence emission peak at 540 nm reached a plateau in about 16 min and maintained stability for a long time.

Kinetic analysis was conducted next. Ten equivalents of GSH, Cys, and Hcy were added into the solutions of **PBD** (10 μ M), respectively. Through monitoring the fluorescence emission at 540 nm, the reactions were found to obey a typical pseudo-first-order and the rate constants were determined to be 0.25 min^{-1} , 0.26 min^{-1} , and 0.20 min^{-1} for GSH, Cys, and Hcy respectively (Figure S5).

Furthermore, we evaluated the pH effect on the sensory response of **PBD** (Figure S3). **PBD** itself was inert to pH change, indicative of the excellent stability of the probe over a broad pH range. By contrast, the probe exhibited a marked fluorescence response to GSH within the pH range 7 to 9, thus enabling detection of biothiols across a relatively wide pH range.

The following experiments of **PBD** were performed in EtOH-PBS buffer (10 mM, pH 7.4, 4:6, *v/v*) and 405 nm was chosen as the excitation wavelength in the fluorescent measurements. For convenience, the fluorescent intensity was recorded at 16 min after the addition of GSH.

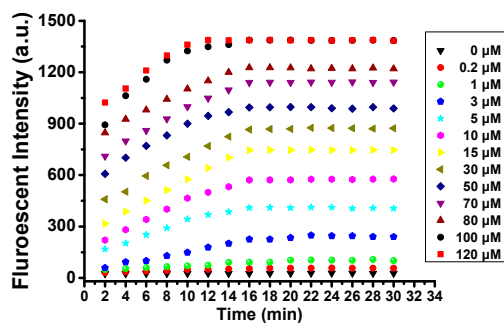


Figure 1. Time-dependent course of the interaction of **PBD** (10 μM) with GSH in EtOH-PBS buffer (Phosphate Buffered Saline) (10 mM, pH 7.4, 4:6, *v/v*). Fluorescence intensity was recorded at 540 nm with $\lambda_{\text{ex}} = 405 \text{ nm}$.

2.2. Sensitivity and Selectivity Studies

Concentration-dependent tests of **PBD** with GSH showed that the fluorescence intensity at 540 nm increased gradually with increasing GSH amounts until a stable signal was reached at 100 μM (Figure 2). The fluorescence enhancement could be about 70-fold when 10 equivalents of GSH were added to the solution of **PBD**. As shown in Figure 2, upon treatment with GSH, the testing solution gave rise to a strong yellow-green fluorescence which is consistent with the emission spectrum of dye **PBOH**. A calibration plot of the signal to the GSH concentrations from 0 μM to 10 μM showed good linearity ($R^2 = 0.9933$), indicating that **PBD** can quantitatively detect GSH within this range. The detection limit of **PBD** toward GSH was found to be 14.5 nM based on the $3\sigma/\text{slope}$ method [39,40], thus enabling a highly sensitive detection of GSH. We also evaluated the response effect of Cys and Hcy to **PBD**. Under the same conditions, **PBD** exhibited similar optical behavior to Cys and Hcy with the detection limits being 17.5 nM and 80.0 nM, respectively (Figure S4).

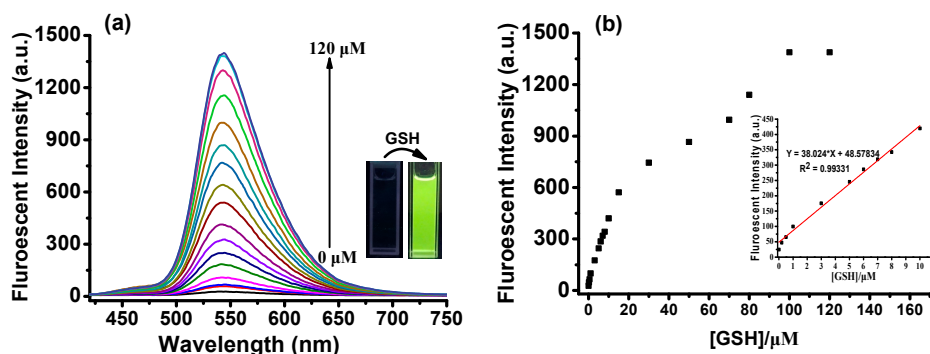


Figure 2. (a) Fluorescence response of **PBD** (10 μM) upon the addition of GSH (0–120 μM) in EtOH-PBS buffer (10 mM, pH 7.4, 4:6, *v/v*). Inset: Fluorescence images of **PBD** (10 μM) in the absence (left) and presence (right) of GSH under a 365 nm UV lamp. (b) Fluorescence intensity of **PBD** (10 μM) at 540 nm as a function of GSH concentration (0–120 μM) in EtOH-PBS buffer (10 mM, pH 7.4, 4:6, *v/v*). Inset: the linear relationship between fluorescence intensity and GSH at low concentrations.

The selectivity of **PBD** for biothiols (100 μM) was evaluated by screening its response to potential competing species (200 μM), including various natural amino acids (Val, Glu, Leu, Met, Asn, Ala, His, Trp, Phe, Ser, Arg, Lys, Gln, Asp, Ile, Thr, Tyr, Pro, and Gly), sulfur species (Na_2S , KSCN , Na_2SO_3 , Na_2SO_4 , $\text{Na}_2\text{S}_2\text{O}_3$, and $\text{Na}_2\text{S}_2\text{O}_4$), oxygen species (H_2O_2), and common salts (KF, NaCl, KBr, KI, Na_2CO_3 , NaHCO_3 , NaNO_2 , NaNO_3 , and AcONa). Figure 3 illustrates that treatment of **PBD** solution with 10 equivalents of GSH resulted in a 70-fold enhancement at 540 nm. Cys gave rise to a similar fluorescence increase. Hcy induced an increment half that of GSH. High concentrations (200 μM) of interfering species induced negligible changes. Following on from this, competition studies were investigated by treating **PBD** with GSH (100 μM) in the presence of 20 equivalents of other

analytes. As shown in Figure 4a,b, addition of GSH to the probe solution resulted in a robust signal enhancement in spite of the coexistence of competing species, demonstrating that probe **PBD** displays strong immunity to interference while sensing biothiols.

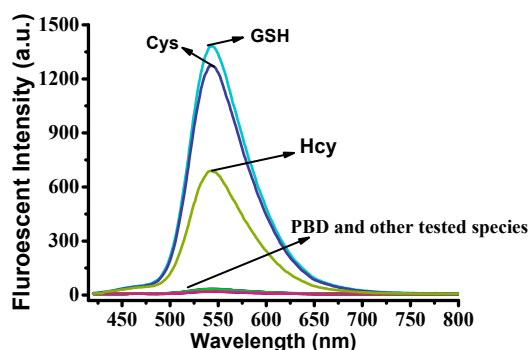


Figure 3. Fluorescence spectra of **PBD** (10 μM) with biothiols (100 μM) and various tested analytes (200 μM). $\lambda_{\text{ex}} = 405 \text{ nm}$.

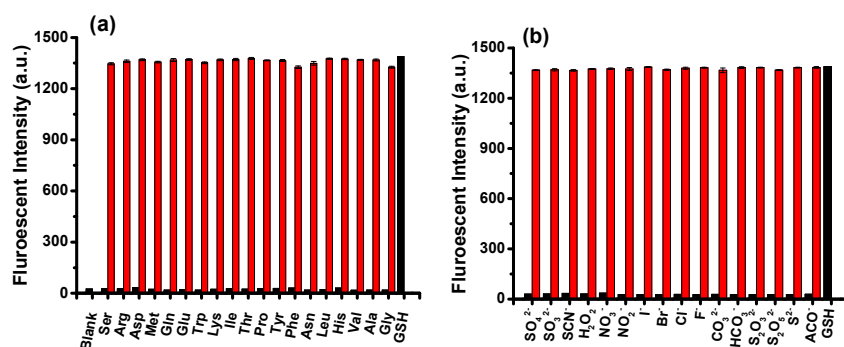
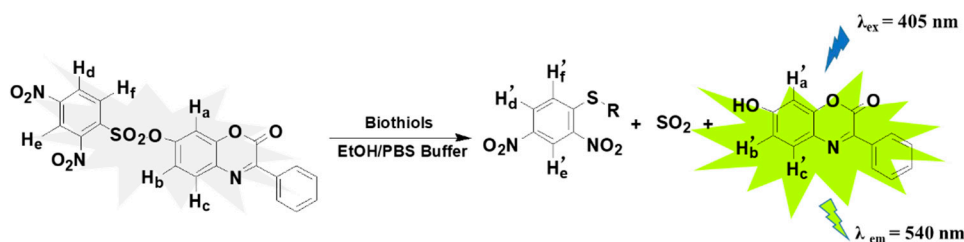


Figure 4. (a,b) Selectivity and competition of **PBD** (10 μM) to **GSH** (100 μM) and other analytes (200 μM). Black bars represent the fluorescence intensity (540 nm) of a single analyte with probe **PBD**. Red bars represent the fluorescence intensity (540 nm) of **PBD** to **GSH** in the presence of various tested analytes. $\lambda_{\text{ex}} = 405 \text{ nm}$.

2.3. Sensing Mechanism Study

The fluorescence turn-on response of **PBD** to biothiols may be attributed to a thiol-anion-mediated $\text{S}_{\text{N}}\text{Ar}$ process which led to the cleavage of 2,4-dinitrophenylsulfonate (Scheme 2). A comparison of the fluorescence spectral profiles of the reaction solution and the precursor compound provides evidence for the proposed mechanism. Upon addition of **GSH** to non-fluorescent **PBD**, a turn-on fluorescent signal at 540 nm was observed and the emission intensity nearly reached the intensity of **PBOH**. In addition, we successfully isolated the fluorescent product of the reaction by column chromatography. As expected, the $^1\text{H-NMR}$ spectrum of the isolated fluorescent product is consistent with that of **PBOH**. Thus, the above results confirmed that dye **PBOH** was released via the cleavage of sulfonate in **PBD** mediated by **GSH**.



Scheme 2. Schematic sensing mechanism of **PBD** toward biothiols.

To confirm the sensing mechanism, we also carried out $^1\text{H-NMR}$ titration experiments to track product formation. After the addition of excessive Cys to **PBD** in $\text{DMSO-}d_6/\text{D}_2\text{O}$ (8/2, v/v), the signals of **PBD** (H_a and H_b) gradually declined. At the same time, three peaks corresponding to the protons (H_a' , H_b' , and H_c') attributable to **PBOH** began to appear, indicating that **PBOH** had been released. With the continuation of this chemical reaction, the signals of **PBOH** (H_a' , H_b' , and H_c') gradually increased. The signals of **PBD** (H_a and H_b) had almost completely disappeared at 20 min. These results demonstrate the cleavage of the DNBS group and the production of fluorophore **PBOH** (Figure 5).

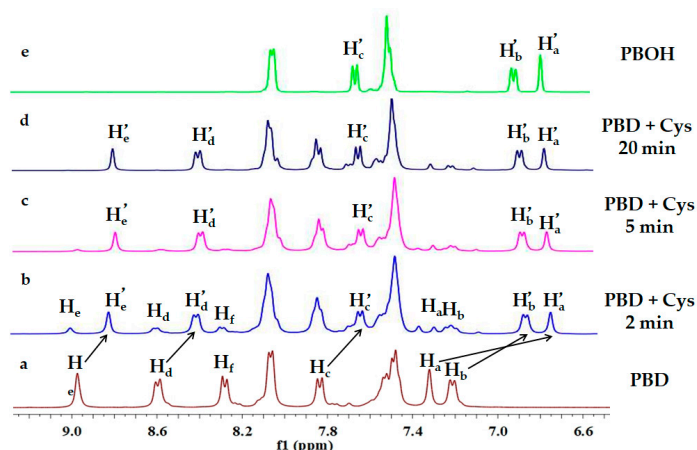


Figure 5. Partial $^1\text{H-NMR}$ spectra of **PBD** before the addition (a) and the change after addition of Cys, 2 min (b), 5 min (c), and 20 min (d), and of **PBOH** (e) in $\text{DMSO-}d_6/\text{D}_2\text{O}$ (8/2, v/v).

To elucidate further the *off-on* sensing mechanism of probe **PBD** towards biothiols, DFT (Density functional theory) calculations were performed. The frontier orbital diagram indicates that the LUMO energy level of DNBS (-3.930 eV) is much lower than that of fluorophore the **PBOH** (-1.021 eV) (Figure 6), which implied that the photo-induced electron transfer (PET) process can happen from the fluorophore moiety to the DNBS group. Owing to the effective fluorescence quenching effect of DNBS, **PBD** is essentially nonfluorescent. After removal of the DNBS group, the fluorescence is recovered.

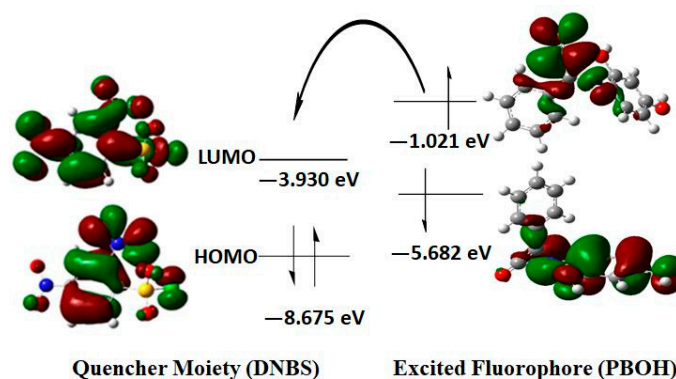


Figure 6. Frontier orbital diagrams of **PBOH** and 2,4-dinitrophenylsulfonyl (DNBS). Orbital energies were calculated using Gaussian 03 program at B3LYP/6-31 g (d, p) level.

2.4. Live Cell Imaging

Having demonstrated its excellent responsiveness and anti-interference in sensing biothiols, we next examined whether **PBD** can be used to detect intracellular thiols in living cells. As shown in Figure 7, after incubating HeLa cells with **PBD** for 20 min, strong yellow-green fluorescence could be observed inside the cells under excitation at 405 nm. In the control experiments, cells were pretreated with *N*-ethylmaleimide (NEM) for 30 min to remove free thiols, and subsequently incubated with

PBD for another 20 min. After being washed with PBS buffer three times, the cells showed almost no fluorescence under a confocal fluorescence microscope. The results showed that **PBD** is cell-permeable and can sense intracellular biothiols in living cells.

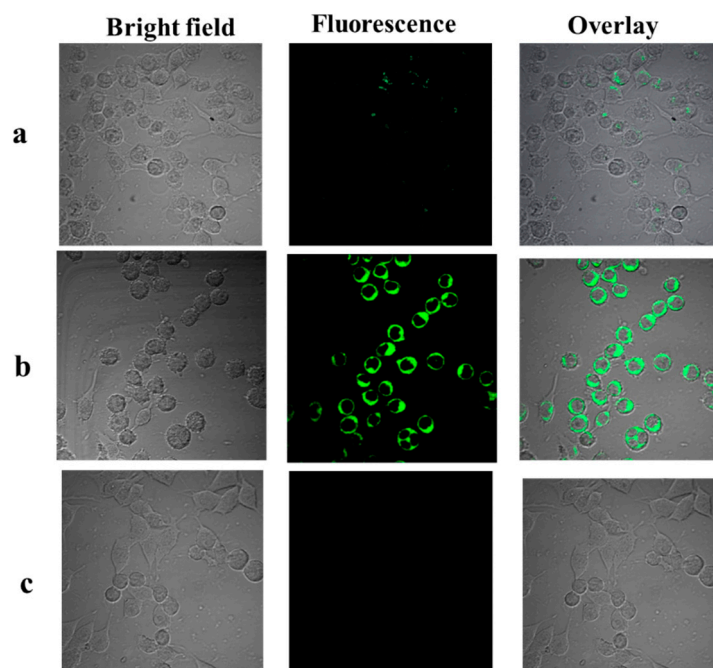


Figure 7. Confocal fluorescence images of HeLa cells. (Left) bright-field image; (middle) fluorescence image; and (right) overlaid image. (a) Cells treated with *N*-ethylmaleimide (NEM) (1 mM) for 30 min followed by incubation with **PBD** (10 μ M) for 20 min. (b) Cells incubated with **PBD** (10 μ M) for 20 min at 37 °C. (c) Untreated cells.

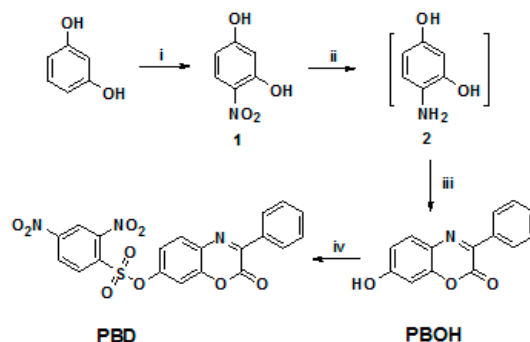
3. Materials and Methods

3.1. Materials.

All chemicals used were of analytical grade and were obtained from commercial suppliers. TLC (Thin-layer chromatography) silica gel plates (GF-254) and silica gel (200-300 mesh) for column chromatography were obtained from Qingdao Marine Chemicals, China. Deionized water was employed throughout all experiments. $^1\text{H-NMR}$ and $^{13}\text{C-NMR}$ spectra were acquired on a Bruker AVANCE II 400 spectrometer (Bruker, Switzerland), respectively. HRMS (High Resolution Mass Spectrometry) spectra were measured with a 6510-Q-TOF spectrometer (Agilent, USA). UV-Visible absorption spectra were recorded by a TU-1901 spectrometer (Beijing, China). Fluorescent measurements were performed on a Lengguang F97Pro FL Spectrophotometer (Shanghai, China). The pH measurement was carried out on a Leici PHS-3C pH meter (Shanghai, China). All spectra were recorded at room temperature.

3.2. Synthesis and Characterization of Compound Information

The four-step synthetic route is outlined in Scheme 3. The details of the synthesis and structural characterization are shown in the Supporting Information (Figures S8–S14).



Scheme 3. Synthesis of **PBD**. Reagents and conditions: (i) fuming HNO_3 , CHCl_3 , and CH_3COOH , r.t.; (ii) Pd/C , H_2 , and $\text{CH}_3\text{COOCH}_2\text{CH}_3$, r.t.; (iii) PhCOCO_2H , EtOH , and CH_3COOH , r.t.; (iv) 2,4-Dinitrobenzenesulfonyl chloride, Et_3N , and THF , r.t.

4. Conclusion

In sum, we have developed a new off-on fluorescent probe **PBD** for biothiols by modifying a fluorescent dye 7-hydroxy-3-phenyl-benzoxazinone with a DNBS unit as a biothiol-specific recognition moiety. In response to biothiols, **PBD** displays significant fluorescence enhancement (up to 70-fold) and a large Stokes shift (155 nm). The probe exhibits a low detection limit as well as excellent selectivity and anti-interference ability toward biothiols over competing species. Finally, this probe has been used to sense biothiols in live HeLa cells.

Supplementary Materials: The supplementary materials are available online.

Author Contributions: B.L. and D.Z. conceived and designed experiments; B.L. performed experiments; B.L. and R.A. analyzed the data; Y.Z. conceived experiments and analyzed the data.

Funding: This study was supported by the Self-Innovation Project for Universities and Institutes of Jinan City (No. 201202035).

Conflicts of Interest: There are no conflicts of interest to declare.

References

- Nadeau, P.J.; Charette, S.J.; Toledano, M.B.; Landry, J. Disulfide Bond-mediated Multimerization of Ask1 and Its Reduction by Thioredoxin-1 Regulate H_2O_2 -induced c-Jun NH_2 -terminal Kinase Activation and Apoptosis. *Mol. Biol. Cell.* **2007**, *18*, 3903–3913. [[CrossRef](#)]
- Requejo, R.; Hurd, T.R.; Costa, N.J.; Murphy, M.P. Cysteine residues exposed on protein surfaces are the dominant intramitochondrial thiol and may protect against oxidative damage. *FEBS J.* **2010**, *277*, 1465–1480. [[CrossRef](#)]
- Ghezzi, P.; Bonetto, V.; Fratelli, M. Thiol–Disulfide Balance: From the Concept of Oxidative Stress to that of Redox Regulation. *Antioxid. Redox. Signal.* **2005**, *7*, 964–972. [[CrossRef](#)]
- Cheng, Z.; Zhang, J.; Ballou, D.P.; Williams, C.H., Jr. Reactivity of Thioredoxin as a Protein Thiol-Disulfide Oxidoreductase. *Chem. Rev.* **2011**, *111*, 5768–5783. [[CrossRef](#)]
- Cross, J.V.; Templeton, D.J. Thiol oxidation of cell signaling proteins: Controlling an apoptotic equilibrium. *J. Cell. Biochem.* **2004**, *93*, 104–111. [[CrossRef](#)]
- Shahrokhian, S. Lead phthalocyanine as a selective carrier for preparation of a cysteine-selective electrode. *Anal. Chem.* **2001**, *73*, 5972–5978. [[CrossRef](#)]
- Seshadri, S.; Beiser, A.; Selhub, J.; Jacques, P.F.; Rosenberg, I.H.; Wilson, W.F.; Wolf, P.A. Plasma homocysteine as a risk factor for dementia and Alzheimer’s disease. *N. Engl. J. Med.* **2002**, *346*, 476–483. [[CrossRef](#)]
- Refsum, H.; Ueland, P.M.; Nygard, O.; Vollset, S.E. Homocysteine and cardiovascular disease. *Annu. Rev. Med.* **1998**, *49*, 31–62. [[CrossRef](#)]
- Lee, J.H.; Sharma, A.; Jang, J.H. Real time OFF–ON monitoring of glutathione (GSH) in living cell. *J. Incl. Phenom. Macro.* **2015**, *82*, 117–122. [[CrossRef](#)]

10. Aoyama, K.; Suh, S.W.; Hamby, A.M.; Liu, J.; Chan, W.Y.; Chen, Y.; Swanson, R.A. Neuronal glutathione deficiency and age-dependent neurodegeneration in the EAAC1 deficient mouse. *Nat. Neurosci.* **2006**, *9*, 119–126. [[CrossRef](#)]
11. Jung, H.S.; Chen, X.; Peng, X. Recent progress in luminescent and colorimetric chemosensors for detection of thiols. *Chem. Soc. Rev.* **2013**, *42*, 6019–6031. [[CrossRef](#)]
12. Lim, S.Y.; Hong, K.H.; Kim, D.I.; Kwon, H.; Kim, H.J. Tunable Heptamethine–Azo Dye Conjugate as an NIR Fluorescent Probe for the Selective Detection of Mitochondrial Glutathione over Cysteine and Homocysteine. *J. Am. Chem. Soc.* **2014**, *136*, 7018–7025. [[CrossRef](#)]
13. Zamfir, L.G.; Rotariu, L.; Bala, C. Sensing of sulfhydryl based compounds by a simple electrochemical approach. *Sens. Actuators B Chem.* **2015**, *206*, 65–73. [[CrossRef](#)]
14. Yin, J.; Hu, Y.; Yoon, J. Fluorescent probes and bioimaging: Alkali metals, alkaline earth metals and pH. *Chem. Soc. Rev.* **2015**, *44*, 4619–4644. [[CrossRef](#)]
15. Farhadi, K.; Forough, M.; Pourhossein, A.; Molaei, R. Highly sensitive and selective colorimetric probe for determination of l-cysteine in aqueous media based on Ag/Pd bimetallic nanoparticles. *Sens. Actuators B Chem.* **2014**, *202*, 993–1001. [[CrossRef](#)]
16. Lee, M.H.; Yang, Z.; Lim, C.W.; Lee, Y.H. Disulfide-cleavage-triggered chemosensors and their biological applications. *Chem. Rev.* **2013**, *113*, 5071–5109. [[CrossRef](#)]
17. Shao, J.H.; Sun, H.; Guo, S.; Ji, J.; Zhao, W. A highly selective red-emitting FRET fluorescent molecular probe derived from BODIPY for the detection of cysteine and homocysteine: An experimental and theoretical study. *Chem. Sci.* **2012**, *3*, 1049–1061. [[CrossRef](#)]
18. Ji, W.; Ji, Y.; Jin, Q.; Tong, Q.; Tang, X. Heavy atom quenched coumarin probes for sensitive and selective detection of biothiols in living cells. *Analyst.* **2015**, *140*, 4379–4383. [[CrossRef](#)]
19. Peng, L.; Zhou, Z.; Wei, R.; Li, K.; Song, K.; Tong, A. A fluorescent probe for thiols based on aggregation-induced emission and its application in live-cell imaging. *Dyes Pigment.* **2014**, *108*, 24–31. [[CrossRef](#)]
20. Shi, J.; Wang, Y.; Tang, X.; Liu, W.; Jiang, H.; Dou, W.; Liu, W. A colorimetric and fluorescent probe for thiols based on 1, 8-naphthalimide and its application for bioimaging. *Dyes Pigment.* **2014**, *100*, 255–260. [[CrossRef](#)]
21. Liu, J.; Sun, Y.Q.; Zhang, H.; Huo, Y.; Shi, Y.; Shi, H.; Guo, W. A carboxylic acid-functionalized coumarin-hemicyanine fluorescent dye and its application to construct a fluorescent probe for selective detection of cysteine over homocysteine and glutathione. *RSC Adv.* **2014**, *4*, 64542–64550. [[CrossRef](#)]
22. Yang, X.F.; Huang, Q.; Zhong, Y.; Li, Z.; Li, H.; Lowry, M.; Strongin, R.M. A dual emission fluorescent probe enables simultaneous detection of glutathione and cysteine/homocysteine. *Chem. Sci.* **2014**, *5*, 2177–2183. [[CrossRef](#)]
23. Niu, L.Y.; Guan, Y.S.; Chen, Y.Z.; Wu, L.Z.; Tung, C.H.; Yang, Q. BODIPY-based ratiometric fluorescent sensor for highly selective detection of glutathione over cysteine and homocysteine. *J. Am. Chem. Soc.* **2012**, *134*, 18928–18931. [[CrossRef](#)]
24. Liu, Y.C.; Xiang, K.Q.; Tian, B.Z. A fluorescein-based fluorescence probe for the fast detection of thiol. *Tetra. Lett.* **2016**, *3*, 2478–2483. [[CrossRef](#)]
25. Zhu, X.Y.; Gao, H.; Zan, W.Y.; Li, Y. A rational designed thiols fluorescence probe: The positional isomer in PET. *Tetrahedron.* **2016**, *72*, 2048–2056. [[CrossRef](#)]
26. Liao, Y.C.; Venkatesan, P.; Wei, L.F.; Wu, S.P. A coumarin-based fluorescent probe for thiols and its application in cell imaging. *Sens. Actuators B Chem.* **2016**, *232*, 732–737. [[CrossRef](#)]
27. Guo, Z.; Nam, S.; Park, S.; Yoon, J. A highly selective ratiometric near-infrared fluorescent cyanine sensor for cysteine with remarkable shift and its application in bioimaging. *Chem. Sci.* **2012**, *3*, 2760–2765. [[CrossRef](#)]
28. Rusin, O.; Luce NN, S.; Agbaria, R. Visual Detection of Cysteine and Homocysteine. *J. Am. Chem. Soc.* **2004**, *2*, 438–439. [[CrossRef](#)]
29. Yang, X.; Guo, Y.; Strongin, R.M. Conjugate Addition/Cyclization Sequence Enables Selective and Simultaneous Fluorescence Detection of Cysteine and Homocysteine. *Angew. Chem. Int. Ed* **2011**, *50*, 10690–10693. [[CrossRef](#)]
30. Lv, H.; Yang, X.F.; Zhong, Y.; Guo, Y.; Li, Z.; Li, H. Native Chemical Ligation Combined with Spirocyclization of Benzopyrylium Dyes for the Ratiometric and Selective Fluorescence Detection of Cysteine and Homocysteine. *Anal. Chem.* **2014**, *3*, 1800–1807. [[CrossRef](#)]

31. Azuma, K.; Suzuki, S.; Uchiyama, S.; Kajiro, T.; Santa, T. A study on the thermal decomposition of KClO₄ and NaClO₄ by acoustic emission thermal analysis. *Photobiol. Sci.* **2003**, *2*, 443–449. [[CrossRef](#)]
32. An, R.B.; Wei, P.; Zhang, D.T.; Su, N. A highly selective 7-hydroxy-3-methyl-benzoxazinone based fluorescent probe for instant detection of thiophenols in environmental samples. *Tetra. Lett.* **2016**, *57*, 3039–3042. [[CrossRef](#)]
33. Manna, S.; Karmakar, P.; Ali, S.S.; Guria, U.N.; Mahapatra, A.K. Michael addition-cyclization-based switch-on fluorescent chemodosimeter for Cysteine and its application in living cell imaging. *New. J. Chem.* **2018**, *42*, 4951–4958. [[CrossRef](#)]
34. Wang, J.; Zhou, C.; Zhang, J.; Zhu, X.; Liu, X.; Wang, Q.; Zhang, H. A new fluorescence turn-on probe for biothiols based on photoinduced electron transfer and its application in living cells. *Spectrochim. Acta. A.* **2016**, *166*, 31–37. [[CrossRef](#)]
35. Dai, X.; Zhang, T.; Miao, J.Y.; Zhao, B.X. A ratiometric fluorescent probe with DNBS group for biothiols in aqueous solution. *Sens. Actuators B Chem.* **2016**, *223*, 274–279. [[CrossRef](#)]
36. Dong, C.; Zhou, C.Q.; Yang, J.W.; Liao, T.C.; Chen, J.X.; Yin, C.X.; Chen, W.H. A novel 3,6-diamino-1,8-naphthalimide derivative as a highly selective fluorescent “turn-on” probe for thiols. *RSC Adv.* **2015**, *5*, 32990–32993. [[CrossRef](#)]
37. Hu, Q.H.; Yu, C.M.; Xi, X.; Wu, S.Z. A fluorescent probe for simultaneous discrimination of GSH and Cys/Hcy in human serum samples via distinctly-separated emissions with independent excitations. *Biosen. Bioelectron.* **2016**, *81*, 341–348. [[CrossRef](#)]
38. Zhang, J.J.; Yu, B.F.; Ning, L.; Zhu, X.Y.; Wang, J.X.; Chen, Z.J.; Liu, X.Y.; Yao, X.J.; Zhang, X.Y.; Zhang, H.X. A Near-Infrared Fluorescence Probe for Thiols Based on Analyte-Specific Cleavage of Carbamate and Its Application in Bioimaging. *Eur. J. Org. Chem.* **2015**, *8*, 1711–1718. [[CrossRef](#)]
39. Chen, W.; Luo, H.; Liu, X.; Foley, J.W.; Song, X. Broadly Applicable Strategy for the Fluorescence Based Detection and Differentiation of Glutathione and Cysteine/Homocysteine: Demonstration in Vitro and in Vivo. *Anal. Chem.* **2016**, *16*, 3638–3646. [[CrossRef](#)]
40. Liu, T.; Huo, F.; Yin, C.; Li, J.; Chao, J.; Zhang, Y. A triphenylamine as a fluorophore and maleimide as a bonding group selective turn-on fluorescent imaging probe for thiols. *Dyes Pigment.* **2016**, *128*, 209–214. [[CrossRef](#)]

Sample Availability: Samples of the compounds PBOH and PBD are not available from the authors.



© 2019 by the authors. Licensee MDPI, Basel, Switzerland. This article is an open access article distributed under the terms and conditions of the Creative Commons Attribution (CC BY) license (<http://creativecommons.org/licenses/by/4.0/>).